NEURAL REGENERATION RESEARCH
www.nrronline.org

Research Article

Unexpected BrdU inhibition on astrocyte-to-neuron conversion

https://doi.org/10.4103/1673-5374.325747
Date of submission: June 28, 2021
Date of decision: August 27, 2021
Date of acceptance: October 27, 2021
Date of web publication: December 10, 2021

Tao Wang[1, #], Jian-Cheng Liao[2, #], Xu Wang[1], Qing-Song Wang[1], Kai-Ying Wan[1], Yi-Yi Yang[1], Qing He[1], Jia-Xuan Zhang[1], Gong Chen[1, *], Wen Li[1, *]

From the Contents

Graphical Abstract *BrdU labeling strategy should be used with great caution when conducting AtN conversion experiments*

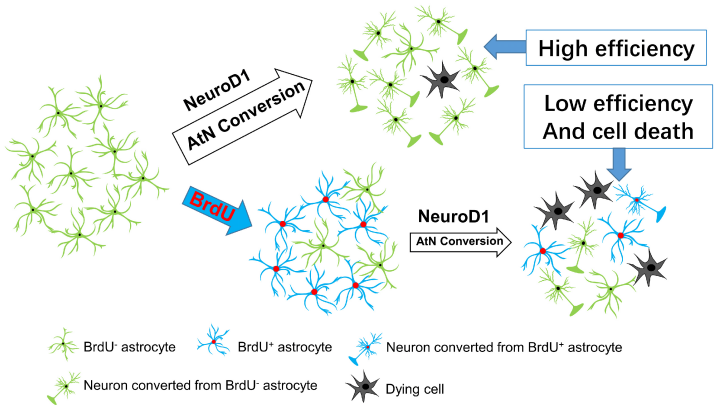

Abstract

5-Bromo-2′-deoxyuridine (BrdU) is a halogenated pyrimidine that can be incorporated into newly synthesized DNA during the S phase of the cell cycle. BrdU is widely used in fate-mapping studies of embryonic and adult neurogenesis to identify newborn neurons, however side effects on neural stem cells and their progeny have been reported. *In vivo* astrocyte-to-neuron (AtN) conversion is a new approach for generating newborn neurons by directly converting endogenous astrocytes into neurons. The BrdU-labeling strategy has been used to trace astrocyte-converted neurons, but whether BrdU has any effect on the AtN conversion is unknown. Here, while conducting a NeuroD1-mediated AtN conversion study using BrdU to label dividing reactive astrocytes following ischemic injury, we accidentally discovered that BrdU inhibited AtN conversion. We initially found a gradual reduction in BrdU-labeled astrocytes during NeuroD1-mediated AtN conversion in the mouse cortex. Although most NeuroD1-infected astrocytes were converted into neurons, the number of BrdU-labeled neurons was surprisingly low. To exclude the possibility that this BrdU inhibition was caused by the ischemic injury, we conducted an *in vitro* AtN conversion study by overexpressing NeuroD1 in cultured cortical astrocytes in the presence or absence of BrdU. Surprisingly, we also found a significantly lower conversion rate and a smaller number of converted neurons in the BrdU-treated group compared with the untreated group. These results revealed an unexpected inhibitory effect of BrdU on AtN conversion, suggesting more caution is needed when using BrdU in AtN conversion studies and in data interpretation.
Key Words: 5-bromo-2′-deoxyuridine; NeuroD1; astrocyte-to-neuron conversion; reprogramming; neural regeneration; reactive astrocytes; neurons; lineage tracing; fate mapping; neural stem cell

Introduction

Neurological disorders such as stroke, Alzheimer's disease, Parkinson's disease, and spinal cord injury, share common pathological features such as loss of neurons and dysfunction of neuronal circuits (Donnan et al., 2008; Shulman et al., 2011; Scheltens et al., 2016; Ahuja et al., 2017). However, the adult mammalian brain and spinal cord have a limited capability to regenerate new neurons, except for a few restricted areas including the sub-ventricular zone in the lateral ventricle and the sub-granular zone in the dental gyrus (Kriegstein and Alvarez-Buylla, 2009; Bond et al., 2015). Unlike neurons, astrocytes in the brain and spinal cord are activated and can divide under disease and injury circumstances (Robel et al., 2011; Burda and Sofroniew, 2014). Recently, it has been reported that resident astrocytes in the mouse striatum and cortex change to neuronal lineage upon injury through

[1]Guangdong-Hong Kong-Macau Institute of CNS Regeneration (GHMICR), Jinan University, Guangzhou, Guangdong Province, China; [2]Department of Neurosurgery, The First Affiliated Hospital of Jinan University, Guangzhou, Guangdong Province, China
*Correspondence to: Wen Li, PhD, liwenhlb@163.com; Gong Chen, PhD, gongchen@jnu.edu.cn.
https://orcid.org/0000-0002-4632-5754 (Wen Li); https://orcid.org/0000-0002-1857-3670 (Gong Chen)
#Both authors contributed equally to this work.

Funding: *This study was supported by the Natural Science Foundation of Guangdong Province of China, Nos. 2021A1515011237 (to WL), 2020A1515010854 (to QSW); the National Natural Science Foundation of China, Nos. U1801681 (to GC), 31701291 (to WL); and the Guangdong Province Science and Technology Planning Project of China, No. 2018B030332001 (to GC).*
How to cite this article: *Wang T, Liao JC, Wang X, Wang QS, Wan KY, Yang YY, He Q, Zhang JX, Chen G, Li W (2022) Unexpected BrdU inhibition on astrocyte-to-neuron conversion. Neural Regen Res 17(7):1526-1534.*

downregulation of Notch signaling or upregulation of achaete-scute family basic helix-loop-helix transcription factor 1 (Ascl1) signaling, but the number and subtype of the newly generated neurons are very limited (Magnusson et al., 2014; Zamboni et al., 2020). During the past decade, our group and other groups have demonstrated that single neural transcription factors including neuronal differentiation 1 (NeuroD1) (Guo et al., 2014; Chen et al., 2020; Liu et al., 2020; Puls et al., 2020; Zhang et al., 2020; Xiang et al., 2021), Ascl1 (Liu et al., 2015), and SRY-box transcription factor 2 (Sox2) (Niu et al., 2013, 2015; Su et al., 2014; Wang et al., 2016) or combinations of factors (Rivetti di Val Cervo et al., 2017; Mattugini et al., 2019; Wu et al., 2020) directly converted reactive astrocytes into neurons of various subtypes through ectopic expression by different viral systems (retrovirus system, lentivirus system, and adeno-associated virus system). Besides the ectopic expression of neural transcription factors, downregulation of polypyrimidine tract binding protein 1 (PTBP1) triggered astrocytes to transdifferentiate into functional neurons in the brain (Qian et al., 2020). More excitingly, this *in vivo* astrocyte-to-neuron (AtN) conversion has been proven in several experimental models of neurological disorders including ischemic stroke, Huntington's disease, and Parkinson's disease, to promote tissue repair, circuit rebuild, and functional recovery (Chen et al., 2020; Qian et al., 2020; Wu et al., 2020; Zhang et al., 2020). One significant study performed on non-human primates demonstrated that NeuroD1-mediated AtN conversion repaired damaged brain tissue after focal ischemic injury (Ge et al., 2020). NeuroD1 belongs to the basic helix-loop-helix transcription factor family, which is transiently expressed in neural progenitor cells (NPCs) during brain development in a variety of brain regions including the cerebral cortex, hippocampus, cerebellum, and olfactory bulb (Ross et al., 2003; Cho and Tsai, 2004; Hevner et al., 2006; Seo et al., 2007). NeuroD1 plays critical roles in terminal neuronal differentiation, maturation, and survival in both embryonic and adult neurogenesis (Gao et al., 2009; Boutin et al., 2010). Recent successful studies in both rodents and non-human primates suggest that *in vivo* AtN conversion is a promising approach for neuroregeneration and repair (Chen et al., 2015; Heinrich et al., 2015; Li and Chen, 2016; Lei et al., 2019).

5-Bromo-2′-deoxyuridine (BrdU) is a thymidine analog that can be incorporated into the genome during the S phase of mitosis (Nowakowski et al., 1989). In neuroscience, it is ubiquitously used to label the proliferative NPCs and their progeny in the study of embryonic and adult neurogenesis. However, its side effects on NPCs and their progeny have also been reported. Earlier studies have demonstrated that the incorporation of BrdU was detrimental to fetal and neonatal development (Garner, 1974; Agnish and Kochhar, 1976; Pollard et al., 1976; Barasch and Bressler, 1977), which was debated by other groups (Miller and Nowakowski, 1988; Hancock et al., 2009; Lehner et al., 2011). Consistently, a significant study performed on macaque monkeys provided substantial evidence that BrdU decreased NPC proliferation and negatively affected the migration and survival of the newly generated neurons when administrated in the fetal stage (Duque and Rakic, 2011). *In vitro* studies also concluded that BrdU inhibits the survival and proliferation of NPCs, and impairs their differentiation into neurons and oligodendrocytes even when administrated at a low dose (Caldwell et al., 2005; Ross et al., 2008; Lehner et al., 2011; Schneider and d'Adda di Fagagna, 2012). Currently, whether BrdU has any effect on AtN conversion is unknown.

In this study, we labeled the proliferative reactive astrocytes with BrdU in the mouse motor cortex after ischemic insult, then used NeuroD1 to induce AtN conversion. When we examined the fate of BrdU-labeled astrocytes during the AtN conversion process, we were surprised that the number of BrdU-labeled astrocytes gradually decreased and very few transdifferentiated into neurons. To avoid complications due to ischemic injury, we used *in vitro* cultured astrocytes to conduct an AtN conversion experiment in the presence or absence of BrdU. The results clearly showed that BrdU reduced the conversion rate and the number of converted neurons. These findings suggest that BrdU inhibits AtN conversion both *in vitro* and *in vivo*.

Materials and Methods

Animals

Thirty adult male wild-type FVB/NJ mice (8–10 weeks old, ~25 g) were used for the *in vivo* experiments. Fifteen postnatal (P0–3) Sprague-Dawley rats were used for isolating primary astrocytes for *in vitro* experiments. Animals were provided by Guangdong Medical Laboratory Animal Center (Guangzhou, Guangdong, China; license No. SCXK (Yue) 2018-0002). The adult mice were housed in groups of three per cage, with ad libitum access to food and water, and maintained in a 12:12-hour light:dark cycle. The study protocol was approved by Jinan University Institutional Animal Care and Use Committee, approval No. IACUC-20180330-06 (March 30, 2018) for the *in vivo* experiments and No. IACUC-20180319-05 (March 19, 2018) for the *in vitro* experiments.

Virus information

For the *in vivo* experiments, single stranded adenovirus-associated viruses were used. A short version of the human glial fibrillary acidic protein (GFAP) promoter (681 bp, provided by PackGene® Biotech, LLC, Guangzhou, Guangdong, China) was used to construct pAAV GFAP::GFP and pAAV GFAP::NeuroD1-P2A-GFP. AAV serotype 9 (AAV9) was produced by PackGene® Biotech, LLC (Guangzhou, China). Iodixanol gradient (Merck/Sigma-Aldrich, St Louis, MO, USA) ultracentrifugation was used for AAV purification. All AAV used in this study was diluted in 0.001% Pluronic F-68 solution (Poloxamer 188 Solution, Caisson Laboratories, Smithfield, UT, USA).

For the *in vitro* experiments, retroviral vectors, CAG::GFP (control retrovirus), and CAG::NeuroD1-IRES-GFP were packaged and concentrated as previously described (Guo et al., 2014). The titer of viral particles was about 1×10^8 transfer units (TU)/mL, which was determined after transduction of HEK293T cells (American Type Culture Collection, Rockville, MD, USA).

Mouse model of ischemic injury and virus injection

Endothelin-1 (ET-1, 1–31, GL Biochem Ltd., Shanghai, China) was used to induce focal ischemic injury by direct injection into the motor cortex of the adult wild-type FVB/NJ mice as previously described (Chen et al., 2020). Briefly, mice were anesthetized by intraperitoneal injection of Avertin (20 mg/kg, 1.25%, Merk/Sigma-Aldrich) and placed in the prone position in the stereotaxic apparatus (RWD, Shenzhen, China), exposing the skull and bregma. Two 0.6-mm holes were drilled in the skull at the coordinates of the forelimb motor cortex (relative to the bregma): + 0.2 mm anterior-posterior (AP), ± 1.5 mm medial-lateral (Roome et al., 2014; Chen et al., 2020). One microliter (1 μg) of ET-1 (1 mg/mL, dissolved in 1x phosphate buffered saline [PBS], osmotic pressure ~320 mOsm/L, pH ~7.3) was injected into each site at –1.3 mm dorsal-ventral from the skull. An infusion pump was used for the injection at a rate of 100 nL/min. After injection, the needle was kept in position for an additional 10 minutes before being slowly withdrawn. As with the ET-1 injection, 1 μL of virus at a concentration of 5×10^{11} GC/mL was injected into the parenchyma in each side 30 days after the ET-1 injection.

Thirty adult animals were initially involved in the experiment, but seven died during BrdU administration and were removed from the experiment. The remaining animals were grouped as follows: NeuroD1 group (injected with AAV9 GFAP::NeuroD1-

P2A-GFP) – three animals each for 4, 10, and 17 days post-injection (DPI); control group (injected with AAV9 GFAP::GFP) – four animals for 4 DPI and five animals each for 10 and 17 DPI.

BrdU administration

In the *in vivo* experiments, BrdU (0.5 g/L, C5138, Merck/Sigma-Aldrich) was administered in the drinking water 2 days after the ET-1 injection for 28 days as described in **Figure 1A**.

In the *in vitro* experiments, 10 μM BrdU was added to the astrocytes and incubated for 24 hours in a 5% CO_2 and 37°C incubator.

Astrocyte culture and *in vitro* AtN conversion

For astrocyte cultures, brains from postnatal (P0–3) rats were collected under cryoanesthesia on ice. Then, cells were dissociated from cortical tissue and plated on 75-cm^2 flasks in astrocyte isolation medium containing Dulbecco's Modified Eagle Medium:F-12 (DMEM/F12) supplemented with 3.5 mM glucose, 10% fetal bovine serum (originating from Australia), and penicillin/streptomycin (all from Thermo Fisher Scientific/Gibco, Grand Island, NY, USA) in a 5% CO_2 and 37°C incubator. When the culture reached 90% confluence, usually taking 7–9 days, the flasks were rigorously shaken overnight and rinsed five times with DMEM/F12 before detachment. The cell culture was dissociated with 0.05% trypsin/ethylenediaminetetraacetic acid (Thermo Fisher Scientific/Gibco) and passaged (P1) at a 1:3 ratio in astrocyte maintenance medium containing DMEM/F12 supplemented with 3.5 mM glucose, 10% fetal bovine serum, 2% B27™ supplement (Thermo Fisher Scientific/Gibco), and penicillin/streptomycin.

For the *in vitro* AtN conversion experiment, P5 astrocyte cultures were used. Approximately 10,000–12,000 cells were plated on poly-D-lysine (Merk/Sigma-Aldrich)-coated glass coverslips (12 mm in diameter, Glaswarenfabrik Karl Hecht GmbH &Co., Sondheim, Germany) in astrocyte maintenance medium and incubated in a 5% CO_2 and 37°C incubator. Retrovirus was added at a dilution of 1:1000 immediately after the BrdU incorporation and removed after overnight infection. Then, the medium was changed to conversion medium containing DMEM/F12 supplemented with 3.5 mM glucose, 1% fetal bovine serum, 2% B27, and penicillin/streptomycin. Three days post-infection, astrocytes from the same batch of the P5 astrocyte culture were added as a feeder layer at a density of 10,000–12,000 cells/well (growth area = 1.9 cm^2). Five days post-infection when neurite-like processes appeared, 200 μg/mL L-ascorbic acid (Merck/Sigma-Aldrich), 1 μM cyclic adenosine monophosphate (Merck/Sigma-Aldrich), 1 μg/mL laminin (Merck/Sigma-Aldrich), 20 ng/mL brain-derived neurotrophic factor (Peprotech, Rocky Hill, NJ, USA), 10 ng/mL neurotrophin-3 (Peprotech), and 10 ng/mL insulin-like growth factor (Peprotech) were added. During the conversion, half the medium was changed every other day.

Immunostaining

For the *in vivo* experiments, animals were injected with an overdose of anesthetic solution (2.5% Avertin), then perfused intracardially with 4% paraformaldehyde. Brain tissues were collected in 4% paraformaldehyde for postfixation overnight, then sequentially incubated in 10%, 20%, and 30% sucrose at 4°C until they sank. The brain was embedded in optimal cutting temperature compound (Tissue-Tek® O.C.T. Compound, Sakura®, Finetek, Torrance, CA, USA) and serially sectioned at the coronal plane in a cryostat (Thermo Scientific, Shanghai, China) at 30-μm thickness. Immunofluorescence staining was performed as previously described (Liu et al., 2020). Briefly, the sections were washed with PBS, then incubated in blocking buffer (5% normal donkey serum, 3% bovine serum albumin, and 0.3% Triton X-100 in PBS) for 1 hour at room temperature. Primary antibodies diluted in blocking solution were added and incubated overnight at 4°C. After sufficient washing with 0.2% PBST (0.2% Tween 20 in PBS), the sections were incubated in donkey anti-mouse/rabbit/rat/chicken secondary antibodies conjugated to Alexa Fluor 488, Alexa Fluor 555, or Alexa Fluor 647 supplemented with 4′,6-diamidino-2-phenylindole (DAPI, F. Hoffmann-La Roche, Natley, NJ, USA) for 2 hours at room temperature. The sections were finally mounted with VECTASHIELD® mounting medium (VECTOR Laboratories, Burlingame, CA, USA). A Zeiss Axioplan fluorescent microscope (Axio Imager Z2, Zeiss, Göttingen, Germany) or confocal microscope (LSM880, Zeiss, Jena, Germany) was used to capture representative pictures.

For the *in vitro* experiments, cells were fixed with 4% paraformaldehyde for 15 minutes at room temperature after three rinses with 0.01 M PBS, and then incubated in 0.01% Triton X-100 for 10 minutes. After three washes with PBS, 3% bovine serum albumin (Merck/Sigma-Aldrich) in PBS was added as blocking buffer for 1 hour, then cells were incubated with the indicated primary antibodies diluted in 1% bovine serum albumin at 4°C overnight. PBST was used to remove the unbound antibodies. Next, secondary antibodies conjugated to fluorochromes were added at a dilution of 1:1000 and incubated for 1 hour at room temperature. Finally, after three PBST washes, 0.5 μg/mL DAPI was added to counterstain the nuclei. The coverslips were mounted on glass slides using anti-fading mounting medium (DAKO, Carpinteria, CA, USA). Apoptosis was analyzed using a One Step terminal deoxynucleotidyl transferase dUTP nick end labeling (TUNEL) assay Kit (Beyotime, Shanghai, China) following the manual. Images were captured with a fluorescence microscope (Axio Imager Z2, Zeiss) for quantification and with a confocal microscope (LSM880, Zeiss) for representative image display.

Detailed information about the primary and secondary antibodies used in the study is listed in **Table 1**.

Data analysis

In vivo experiments: Images acquired at 400× magnification (212.6 μm × 212.6 μm) by a confocal microscope (LSM880, Zeiss) were used for cell counting by Zeiss ZEN 2.3 software (blue edition, Göttingen, Germany). For quantitation, positive signals (including BrdU, GFP, neuronal marker NeuN, astrocyte marker GFAP, and nuclear marker DAPI) were acquired from 15 random fields chosen from three brain slices (five fields/brain slice) of one animal. Three to five animals were used. Cell number/mm^2 was calculated as the number of cells of interest per field (400× magnification of LSM 880) divided by the area of the field (212.6 μm × 212.6 μm).

In vitro experiments: Quantification of immunostaining was performed by Zeiss ZEN 2.3 software (blue edition, Göttingen, Germany) using images captured at 200× magnification (464.9 μm × 464.9 μm) by a fluorescence microscope (Axio Imager Z2, Zeiss). Parameters for image capturing and post-analysis were adjusted to the same values for each antigen tested. For quantitative analysis of specific positive signals (including BrdU, GFP for infected cells, astrocyte markers GFAP and S100β, neuronal markers TuJ1 and NeuN, NeuroD1, and TUNEL-positive signal), 15–20 random fields per coverslip were chosen and 3–4 coverslips were used per cell batch. Three cell batches isolated in three independent experiments were used. NeuroD1 signal intensity in the infected cells (GFP^+ cells) was measured by Zeiss ZEN 2.3 software, and 150 cells of each cell batch were analyzed. Three cell batches were used. For the analysis of cell number changes during *in vitro* AtN conversion, images of live cells were captured by an inverted fluorescence microscope (Zeiss Axio Observer A1) at 100× magnification (929.79 μm × 929.79 μm). Five randomly chosen fields were of three cell batches.

Table 1 | **Antibodies for immunostaining**

Antibodies	Company	Identifier	RRID	Working dilution
Guinea pig anti-NeuN	Merck/Millipore, Temecula, CA, USA	Cat# ABN90	AB11205592	1:1000
Rabbit anti-NeuN	Merck/Millipore	Cat# ABN78	AB10807945	1:1000
Mouse anti-TuJ1	Merck/Sigma-Aldrich, St. Louis, MO, USA	Cat# T8660	AB477590	1:1000
Rat anti-GFAP	Thermo Fisher Scientific, Eugene, OR, USA	Cat# 13-003	NA	1:1000
Mouse anti-GFAP	Merck/Sigma-Aldrich	Cat# G3893	AB477010	1:1000
Rabbit anti-S100β	Abcam, Cambridge, UK	Cat# ab52642	AB882426	1:500
Mouse anti-NeuroD1	Abcam	Cat# ab60704	AB943491	*In vivo* 1:500 *In vitro* 1:1000
Rat anti-BrdU	Abcam	Cat# ab6326	AB305426	0.736111111
Chicken anti-GFP	Abcam	Cat# ab13970	AB300798	*In vivo* 1:1000 *In vitro* 1:5000
Donkey anti-mouse Alexa Fluor 488	Thermo Fisher Scientific	Cat# A21202	AB141607	1:1000
Donkey anti-rabbit Alexa Fluor 488	Thermo Fisher Scientific	Cat# A21206	AB2535792	1:1000
Goat anti-chicken Alexa Fluor 488	Thermo Fisher Scientific	Cat# A11039	AB2534096	1:1000
Donkey anti-rabbit Alexa Fluor 555	Thermo Fisher Scientific	Cat# A31572	AB162543	1:1000
Donkey anti-mouse Alexa Fluor 555	Thermo Fisher Scientific	Cat# A31570	AB2536180	1:1000
Donkey anti-mouse Alexa Fluor 647	Thermo Fisher Scientific	Cat# A31571	AB162542	1:1000
Goat anti-rat Alexa Fluor 647	Thermo Fisher Scientific	Cat# A21247	AB141778	1:1000
Donkey anti-rabbit Alexa Fluor 647	Thermo Fisher Scientific	Cat# A31573	AB2536183	1:1000

BrdU: 5′-Bromo-2′-deoxyuridine; GFAP: glial fibrillary acidic protein; GFP: green fluorescent protein; NA: not applicable; NeuN: neuronal nuclei; TuJ1: neuron-specific class III beta-tubulin.

Statistical analysis

No statistical methods were used to predetermine sample sizes; however, our sample sizes are similar to those reported in a previous publication (Chen et al., 2020). Data are presented as mean ± standard deviation (SD) (*in vivo* experiments) or mean ± standard error for the mean (SEM) (*in vitro* experiments). Paired Student's *t*-test and one-way analysis of variance, followed by Tukey's multiple comparison test, or two-way analysis of variance, followed by Sidak's multiple comparison test were used for statistical analysis (GraphPad Prism 7, GraphPad Software Inc., San Diego, CA, USA). Double-blinded statistics were performed in most data analyses. $P < 0.05$ was considered statistically significant.

Results

AtN conversion after BrdU labeling

Our group and other groups have demonstrated that reactive astrocytes can be directly converted into neurons by ectopically expressing neural transcription factors or knocking down PTBP1, leading to tissue and function repair of the injured brain (Rivetti di Val Cervo et al., 2017; Chen et al., 2020; Qian et al., 2020; Wu et al., 2020). However, this *in vivo* AtN conversion has been challenged recently owing to confusion largely caused by a high dose of AAV used in some studies that inevitably led to a so called "leakage" of the transgene signal directly into neurons near the targeted glial cells (Wang et al., 2020). Another concern was raised on the basis of a BrdU incorporation experiment in which the number of BrdU-labeled neurons was very small after *in vivo* AtN conversion (Wang et al., 2020). To investigate why few BrdU-labeled neurons remained after conversion, we established ET-1-induced ischemic injury in the FVB mouse motor cortex and continuously administrated BrdU in the drinking water to label dividing glial cells (**Figure 1A**). At 30 days after the injury (continuous 28-day BrdU administration), AAV9 GFAP::NeuroD1-P2A-GFP was injected into the injured cortical region and animals were sacrificed for analysis at 4, 10, and 17 days after virus infection (DPI) (**Figure 1A**). Similar to our previous study (Chen et al., 2020), NeuroD1 expression was detected in astrocytes at 4 DPI (**Figure 1B**, top row) and the NeuroD1-GFP-infected cells gradually changed from $GFAP^+$ astrocytes to $NeuN^+$ neurons from 4 to 17 DPI (**Figure 1B**). Quantitation showed that the NeuN signal in the infected cells increased from 41% at 4 DPI to 73% at 17 DPI, while the GFAP signal decreased concomitantly from 69% at 4 DPI to 19% at 17 DPI (**Figure 1C**). These results suggest efficient AtN conversion occurred in the ET-1-induced chronic ischemic injury model in the mouse motor cortex.

Analysis of the number of BrdU-labeled cells during the conversion revealed that the proportion of both BrdU-positive astrocytes and the total BrdU-positive cells among the NeuroD1-GFP-infected cells gradually decreased (**Figure 2A**). Namely, the ratio of BrdU-positive astrocytes among the NeuroD1-GFP-infected cells declined from 32% at 4 DPI to 13% at 17 DPI ($P = 0.0012$ for 4 DPI *vs*. 10 DPI, $P = 0.0006$ for 4 DPI *vs*. 17 DPI; **Figure 2B** and **C**). Similarly, among the $GFAP^+$ astrocytes, the ratio of BrdU-positive astrocytes also decreased from 75% at 4 DPI to 49% at 17 DPI ($P = 0.015$; **Figure 2D**). This phenomenon indicated a gradual loss of BrdU-labeled cells during NeuroD1-induced AtN conversion. We then investigated whether this reduction is specifically related to NeuroD1 by infecting the astrocytes with a control AAV GFAP::GFP. Surprisingly, the proportion of BrdU-labeled astrocytes did not show a significant change among the GFP-infected cells, suggesting that BrdU did not affect normal dividing glial cells (**Figure 2E–G**). Therefore, the reduction in BrdU-positive cells in the NeuroD1 group is potentially linked to the AtN conversion.

Very few BrdU-labeled neurons are observed after AtN conversion

Because the ratio of BrdU-labeled astrocytes decreased among the NeuroD1-GFP-infected cells, we wondered whether this portion of astrocytes can transdifferentiate into neurons. To answer this question, we examined the BrdU-positive neurons within the NeuroD1-converted neurons at different stages of AtN conversion. At 4 DPI, the expression of NeuroD1 was clearly observed in BrdU-positive astrocytes (**Figure 3A**), suggesting that incorporation of BrdU into the astrocytes did not affect NeuroD1 expression. As the neuronal reprogramming proceeded, we detected both BrdU-positive and negative neurons ($NeuN^+$) among the NeuroD1-GFP-infected cells (**Figure 3B**), but the ratio was dramatically different. Strikingly, at the indicated time points during AtN conversion, BrdU-positive neurons only constituted a very small portion of the total NeuroD1-converted neurons (**Figure 3C** and **D**). Namely, most of the converted neurons were BrdU-negative, raising the question whether BrdU had any negative effect on the neuronal conversion process.

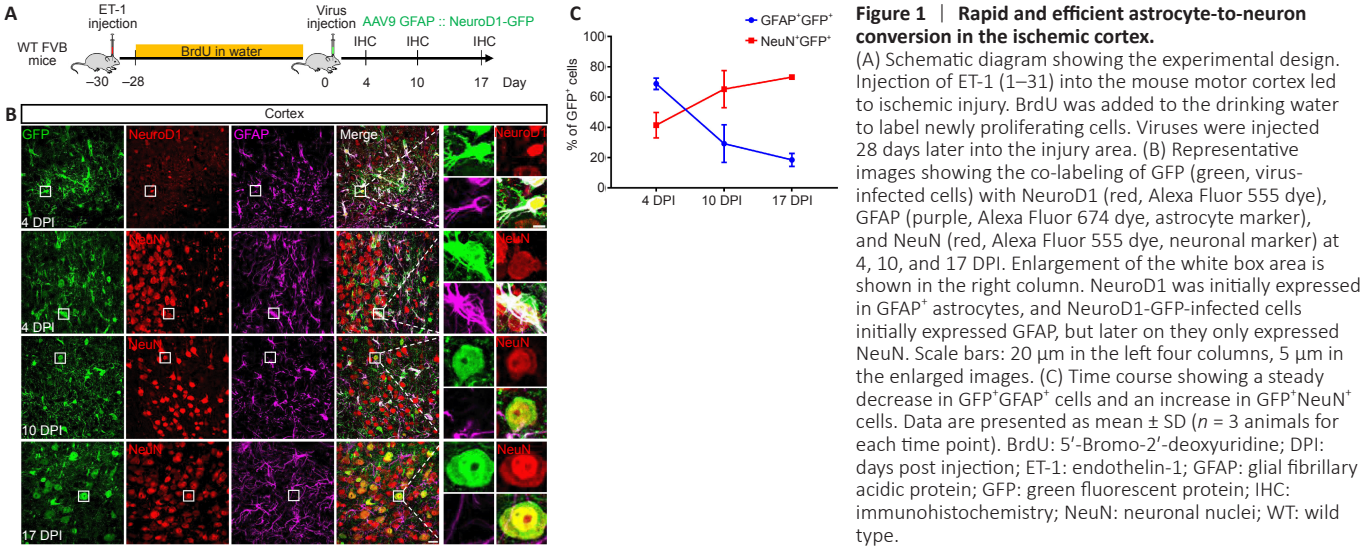

Figure 1 | Rapid and efficient astrocyte-to-neuron conversion in the ischemic cortex.
(A) Schematic diagram showing the experimental design. Injection of ET-1 (1–31) into the mouse motor cortex led to ischemic injury. BrdU was added to the drinking water to label newly proliferating cells. Viruses were injected 28 days later into the injury area. (B) Representative images showing the co-labeling of GFP (green, virus-infected cells) with NeuroD1 (red, Alexa Fluor 555 dye), GFAP (purple, Alexa Fluor 674 dye, astrocyte marker), and NeuN (red, Alexa Fluor 555 dye, neuronal marker) at 4, 10, and 17 DPI. Enlargement of the white box area is shown in the right column. NeuroD1 was initially expressed in GFAP$^+$ astrocytes, and NeuroD1-GFP-infected cells initially expressed GFAP, but later on they only expressed NeuN. Scale bars: 20 μm in the left four columns, 5 μm in the enlarged images. (C) Time course showing a steady decrease in GFP$^+$GFAP$^+$ cells and an increase in GFP$^+$NeuN$^+$ cells. Data are presented as mean ± SD (n = 3 animals for each time point). BrdU: 5′-Bromo-2′-deoxyuridine; DPI: days post injection; ET-1: endothelin-1; GFAP: glial fibrillary acidic protein; GFP: green fluorescent protein; IHC: immunohistochemistry; NeuN: neuronal nuclei; WT: wild type.

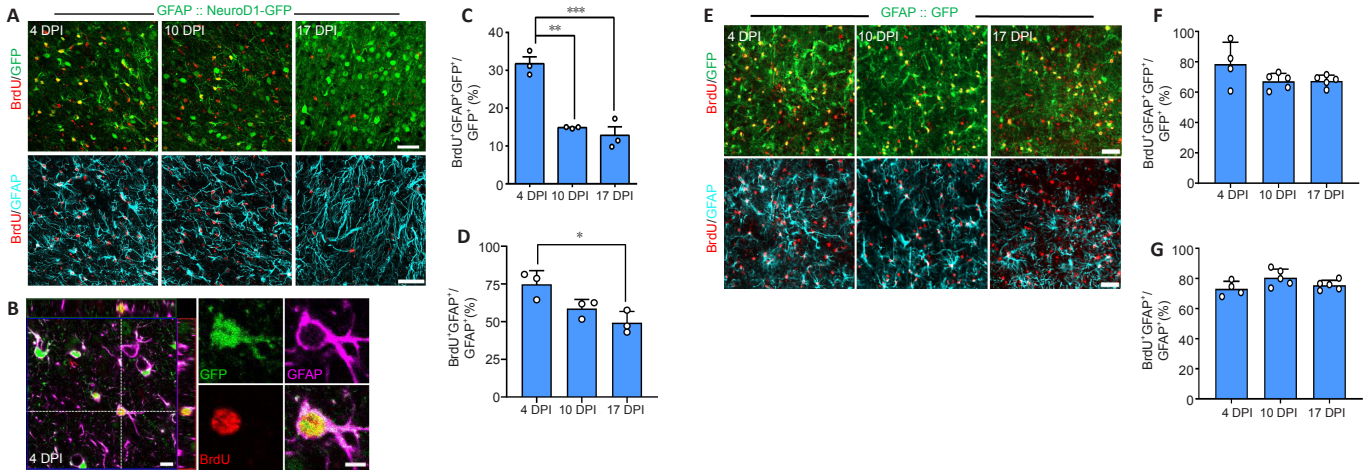

Figure 2 | Decrease in BrdU-positive cells during astrocyte-to-neuron conversion.
(A) Representative images showing a gradual decrease in BrdU-positive (red, Alexa Fluor 555 dye) cells in AAV9 GFAP::NeuroD1-GFP-infected areas (green for GFP-infected cells; cyan for astrocyte marker GFAP, Alexa Fluor 647 dye). (B) Representative images showing the co-labeling of NeuroD1-GFP-infected cells (green) with the astrocyte marker (GFAP, purple, Alexa Fluor 647 dye) and BrdU (red, Alexa Fluor 555 dye) at 4 DPI. The cell at the cross of the white dashed lines is enlarged on the right. (C) Quantification showing that the proportion of BrdU-labeled astrocytes among the NeuroD1-GFP-infected cells (BrdU$^+$GFAP$^+$GFP$^+$ cells) gradually decreased from 4 to 17 DPI (**P = 0.0012, ***P = 0.0006, one-way analysis of variance followed by Tukey's multiple comparison test, n = 3 animals for each time point). (D) Quantification showing that the proportion of BrdU-labeled astrocytes (BrdU$^+$GFAP$^+$ cells) also gradually decreased from 4 to 17 DPI (*P = 0.0149, one-way analysis of variance followed by Tukey's multiple comparison test, n = 3 animals for each time point). (E) Representative images illustrating BrdU-labeled cells in the control group (GFAP::GFP). Red for BrdU (Alexa Fluor 555 dye); green for GFP; cyan for astrocyte marker GFAP (Alexa Fluor 647 dye). Scale bars: 50 μm in A and E, 10 and 5 μm in B (left and right panels, respectively). (F, G) Quantitative analysis showing no significant changes from 4 to 17 DPI after GFP virus injection (one-way analysis of variance followed by Tukey's multiple comparison test, n = 4 animals for 4 DPI and n = 5 for 10 and 17 DPI). Data are presented as mean ± SD. BrdU: 5′-Bromo-2′-deoxyuridine; DPI: days post injection; GFAP: glial fibrillary acidic protein; GFP: green fluorescent protein.

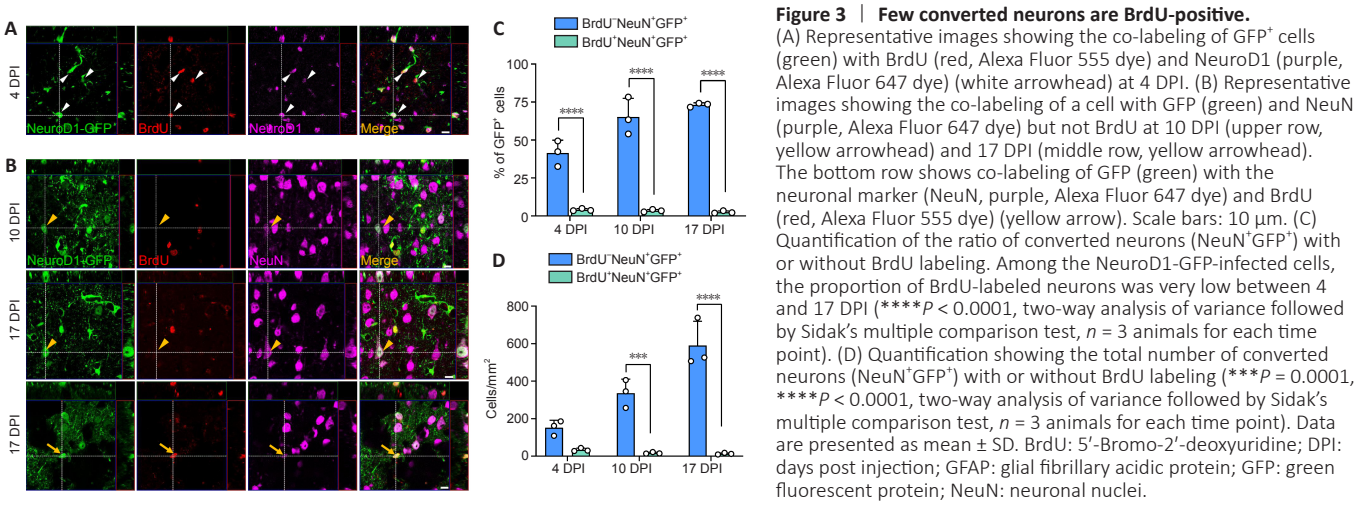

Figure 3 | Few converted neurons are BrdU-positive.
(A) Representative images showing the co-labeling of GFP$^+$ cells (green) with BrdU (red, Alexa Fluor 555 dye) and NeuroD1 (purple, Alexa Fluor 647 dye) (white arrowhead) at 4 DPI. (B) Representative images showing the co-labeling of a cell with GFP (green) and NeuN (purple, Alexa Fluor 647 dye) but not BrdU at 10 DPI (upper row, yellow arrowhead) and 17 DPI (middle row, yellow arrowhead). The bottom row shows co-labeling of GFP (green) with the neuronal marker (NeuN, purple, Alexa Fluor 647 dye) and BrdU (red, Alexa Fluor 555 dye) (yellow arrow). Scale bars: 10 μm. (C) Quantification of the ratio of converted neurons (NeuN$^+$GFP$^+$) with or without BrdU labeling. Among the NeuroD1-GFP-infected cells, the proportion of BrdU-labeled neurons was very low between 4 and 17 DPI (****P < 0.0001, two-way analysis of variance followed by Sidak's multiple comparison test, n = 3 animals for each time point). (D) Quantification showing the total number of converted neurons (NeuN$^+$GFP$^+$) with or without BrdU labeling (***P = 0.0001, ****P < 0.0001, two-way analysis of variance followed by Sidak's multiple comparison test, n = 3 animals for each time point). Data are presented as mean ± SD. BrdU: 5′-Bromo-2′-deoxyuridine; DPI: days post injection; GFAP: glial fibrillary acidic protein; GFP: green fluorescent protein; NeuN: neuronal nuclei.

BrdU impairs NeuroD1-induced AtN conversion *in vitro*

To investigate whether BrdU affects NeuroD1-induced AtN conversion and avoid potential complications induced by ET-1 ischemic injury, we performed *in vitro* neuronal conversion experiments using cultured astrocytes in the presence or absence of BrdU. Previous studies have demonstrated that 10 μM BrdU was not toxic to astrocytes and could label ~70% of astrocytes after a short incubation time (Caldwell et al., 2005; Lehner et al., 2011; Schneider and d'Adda di Fagagna, 2012; Zhang et al., 2015). Thus, we performed a 24-hour incubation of 10 μM BrdU with primary cultured rat astrocytes (**Figure 4A**). The results showed that ~70% of astrocytes were labeled with BrdU after the treatment (**Figure 4B** and **C**), suggesting a robust proliferation of the primary rat astrocytes within 24 hours. When cultured rat astrocytes were infected with control retrovirus CAG::GFP, most infected cells were astrocytes and no TuJ1$^+$ neurons were observed by 14 DPI (**Figure 4D**), suggesting no contaminated neural stem cells within the primary rat astrocyte culture. When retrovirus CAG::NeuroD1-IRES-GFP was used on the primary rat astrocytes without or with BrdU treatment, we observed a sharp contrast between the two groups (**Figure 4E**). In the group without BrdU treatment, most of the infected astrocytes expressed NeuroD1 and were successfully converted into neuron-like cells at 7 DPI (**Figure 4E**, top row). However, in the group with BrdU treatment, a significant portion of the infected cells were astrocytes, with relatively strong GFAP expression and weak NeuroD1 expression (**Figure 4E** and **F**, bottom row, NeuroD1 intensity in the infected cells at 7 DPI: $P = 0.01$).

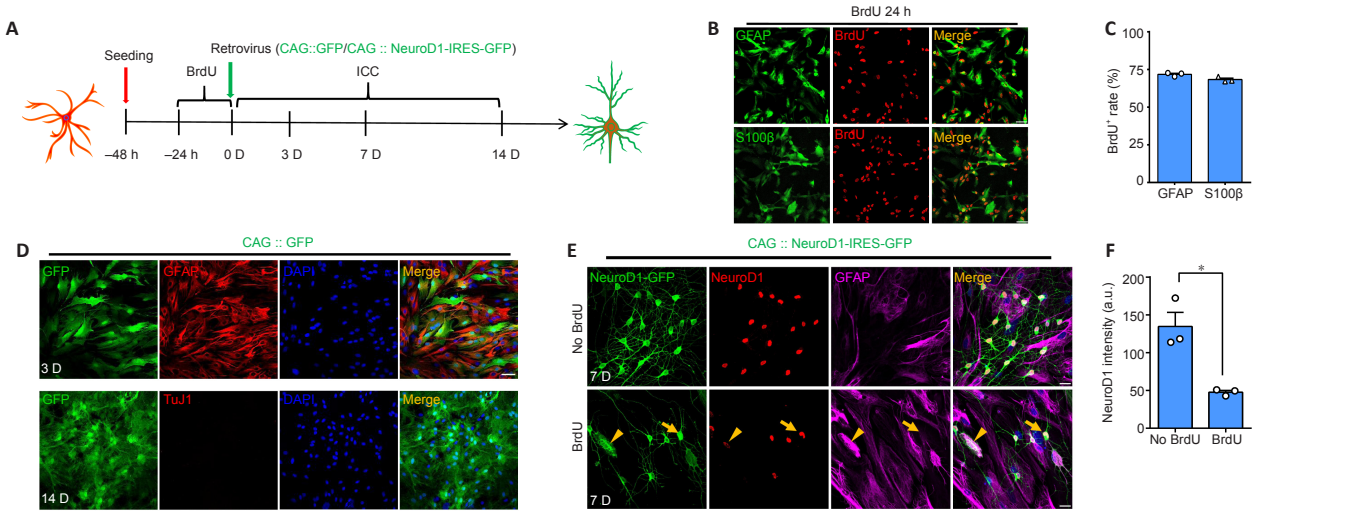

Figure 4 | **Efficient BrdU labeling of primary rat astrocytes *in vitro*.**

(A) Schematic diagram showing the experimental design. (B) Representative images showing co-labeling of the two astrocyte markers GFAP and S100β (green, Alexa Fluor 488 dye) with BrdU (red, Alexa Fluor 555 dye) after incubation with BrdU for 24 hours. (C) Quantitative analysis showed that BrdU$^+$GFAP$^+$ or BrdU$^+$S100β$^+$ cells accounted for about 70% of the cultured astrocytes ($n = 3$ independent experiments with different batches of primary cells). (D) Representative images showing that the control GFP-infected cells were GFAP$^+$ astrocytes (red, Alexa Fluor 555 dye), with no contamination of TuJ1$^+$ neurons. (E) Representative images showing that NeuroD1-GFP-infected cells expressed NeuroD1 (red, Alexa Fluor 555 dye), but the intensity of NeuroD1 (yellow arrowheads) was reduced in the BrdU group (bottom row). Scale bars: 50 μm. (F) Quantitation showed a weaker NeuroD1 expression level in the infected cells treated with BrdU compared with that in the untreated cells (*$P = 0.041$, paired Student's *t*-test; $n = 3$ independent experiments with different batches of primary cells). Data are presented as mean ± SEM. a.u.: Arbitrary unit; BrdU: 5′-bromo-2′-deoxyuridine; DAPI: 4′,6-diamidino-2-phenylindole; GFAP: glial fibrillary acidic protein; GFP: green fluorescent protein; ICC: immunocytochemistry; IRES: internal ribosome entry sit; TuJ1: neuron-specific class III beta-tubulin.

We next examined the effect of BrdU on AtN conversion by comparing the NeuN signal between BrdU-treated and untreated astrocytes at 7 and 14 DPI following NeuroD1-GFP retroviral infection (**Figure 5**). In the control group without BrdU treatment, most of the NeuroD1-GFP-infected cells showed a NeuN signal at 7 DPI (**Figure 5A**, top row). However, in the BrdU-treated group, the NeuN signal was very weak among the NeuroD1-GFP-infected cells at 7 DPI (**Figure 5A**, bottom row). Quantitative analysis showed that without BrdU treatment, NeuroD1 rapidly converted astrocytes into NeuN$^+$ neurons at the high conversion rate of 85% at 7 DPI (**Figure 5B**). However, in the BrdU-treatment group, the AtN conversion rate dramatically dropped to below 40% ($P < 0.0001$; **Figure 5B**). Interestingly, in the BrdU-treatment group, a small portion of astrocytes were not labeled with BrdU (around ~30%), and the AtN conversion rate of these cells (BrdU negative, 34%) was higher than that of the BrdU-positive cells (16%, $P = 0.0002$). At the later stage of AtN conversion (14 DPI), although the conversion rate increased in both groups, the conversion rate in the BrdU-treatment group remained much lower than that of the non-BrdU group (**Figure 5C** and **D**). In addition to the conversion rate decrease induced by BrdU treatment, the number of converted neurons in the BrdU-treatment group was significantly lower than that in the group without BrdU treatment at both 7 and 14 DPI (**Figure 5E** and **F**).

Previous studies have reported toxic effects of BrdU on neural stem cells and neuronal differentiation (Caldwell et al., 2005; Ross et al., 2008; Duque and Rakic, 2011; Lehner et al., 2011; Schneider and d'Adda di Fagagna, 2012). Our findings suggest that BrdU has similar toxic effects on AtN conversion. To further analyze the BrdU effect, we investigated the cell number change during AtN conversion. In the control group where astrocytes were infected with GFP alone, no significant difference "existed between" the BrdU-treated and untreated astrocytes (**Figure 6A** and **B**). However, when the astrocytes were infected with the NeuroD1 virus, a dramatic cell morphology switch from astrocyte-like to neuron-like morphology was observed together with a steady cell number decrease, suggesting that some cells did not survive "during" this drastic cell conversion change (**Figure 6A** and **B**). Interestingly, the BrdU-treated group showed an even higher cell loss compared with that in the untreated group (**Figure 6B**; 7 DPI: $P = 0.032$; 9 DPI: $P = 0.046$). Next, we performed TUNEL staining to examine whether this cell loss during AtN conversion was partly due to apoptosis as previously reported (Gascón et al., 2016). A TUNEL-positive signal was observed in both the BrdU-treated and untreated groups at 7 DPI after NeuroD1 transduction. However, the TUNEL-positive signal in the BrdU-treated group was significantly higher than that in the untreated group ($P = 0.043$, paired Student's *t*-test; **Figure 6C** and **D**).

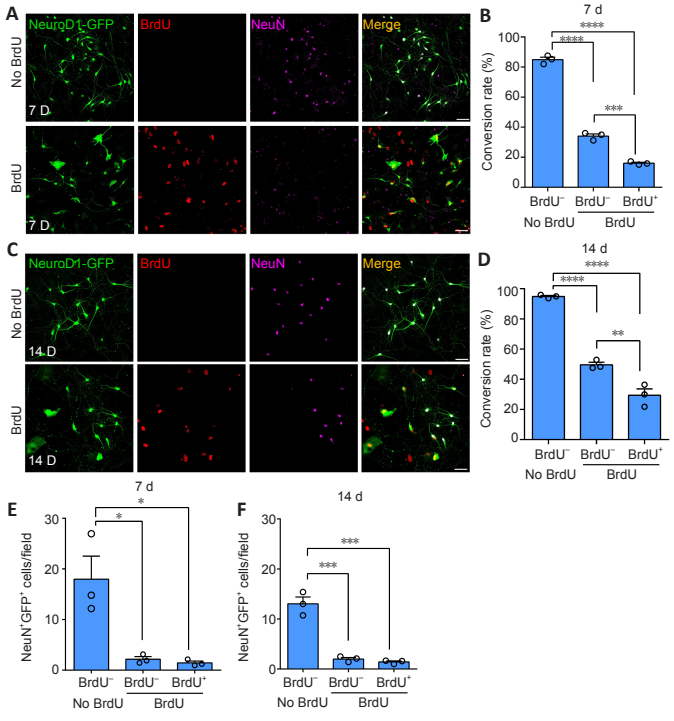

Figure 5 | BrdU impaires astrocyte-to-neuron conversion *in vitro*.
(A) Comparison between NeuroD1-GFP-infected cells with or without BrdU treatment revealed a sharp contrast in NeuN staining at 7 DPI. Representative images showing the co-staining of GFP$^+$ (green) cells with BrdU (red, Alexa Fluor 555 dye) and NeuN (purple, Alexa Fluor 647 dye) at 7 days in the groups without (top row) and with BrdU treatment (bottom row). (B) Quantified data showing a significant reduction in conversion efficiency in the BrdU group. Even in the BrdU-treated group, the proportion of BrdU$^+$ neurons was significantly lower than the proportion of BrdU$^-$ neurons. ***P = 0.0002, ****P < 0.0001; one-way analysis of variance followed by Tukey's multiple comparison test; n = 3 independent experiments with different batches of primary cells. (C) Representative images showing the co-labeling of NeuroD1-GFP-infected cells (green) with BrdU (red, Alexa Fluor 555 dye) and NeuN (purple, Alexa Fluor 647 dye) at 14 DPI. Scale bar: 50 µm. (D) Quantified data showing the reduction in conversion efficiency in the BrdU group at 14 DPI. **P = 0.0042, ****P < 0.0001; one-way analysis of variance followed by Tukey's multiple comparison test; n = 3 independent experiments with different batches of primary cells. (E, F) Total number of converted neurons also showed a significant reduction in the BrdU group at both 7 (E) and 14 (F) DPI. *P < 0.05; ***P < 0.001, one-way analysis of variance followed by Tukey's multiple comparison test; n = 3 independent experiments with different batches of primary cells. Data are presented as mean ± SEM. BrdU: 5′-Bromo-2′-deoxyuridine; GFP: green fluorescent protein; NeuN: neuronal nuclei.

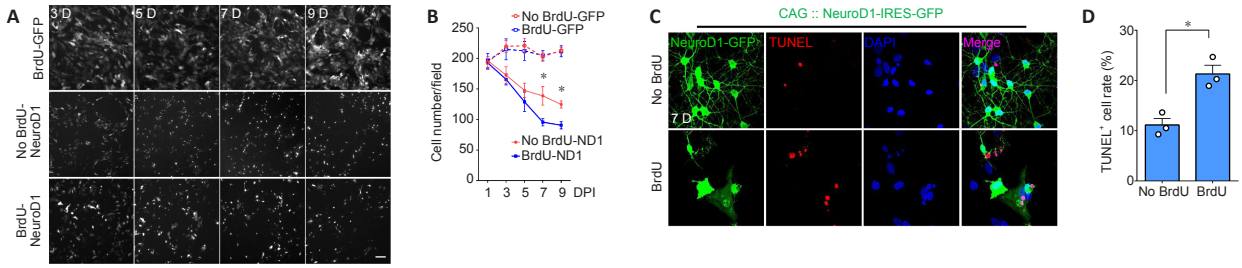

Figure 6 | BrdU exacerbates cell death during astrocyte-to-neuron conversion.
(A) Representative images showing the cell number and morphology changes during AtN conversion. The GFP signal (white) was captured from live cells at different time points of AtN conversion. The upper row is BrdU-treated astrocytes infected with the control GFP virus, the middle row is NeuroD1-infected cells without BrdU treatment, and the bottom row is NeuroD1-infected cells treated with BrdU. (B) Quantification of cell numbers during AtN conversion. BrdU exacerbated cell loss during AtN conversion (*P = 0.032 at 7 DPI and *P = 0.046 at 9 DPI, two-way analysis of variance followed by Sidak's multiple comparison test. n = 3 independent experiments with different batches of primary cells). (C) Representative pictures showing the TUNEL signal (red, Cy3) in condensed nuclei (DAPI, blue) at 7 DPI after NeuroD1 infection. Scale bars: 100 µm in A, 20 µm in C. (D) Quantitative analysis showing that the TUNEL signal increased in the BrdU-treated group at 7 DPI after NeuroD1 infection, suggesting exacerbated cell death induced by BrdU during AtN conversion (*P = 0.043, paired Student's t-test; n = 3 independent experiments with different batches of primary cells). Data are presented as mean ± SEM. BrdU: 5′-Bromo-2′-deoxyuridine; DAPI: 4′,6-diamidino-2-phenylindole; GFP: green fluorescent protein; IRES: internal ribosome entry site; TUNEL: terminal deoxynucleotidyl transferase dUTP nick end labeling.

Taken together, these results suggest that the incorporation of BrdU into the genomic backbone of astrocytes impairs the AtN conversion by exacerbating cell death during the course of cell fate change.

Discussion

In this study, we intended to label dividing reactive astrocytes with BrdU and track their cell fate after neuronal conversion. However, we made the unexpected discovery that BrdU inhibited AtN conversion in an ischemic injury model in the mouse cortex *in vivo*. We wondered whether this unexpected BrdU inhibition was associated with the ischemic insult. Because normal astrocytes in the adult mammalian brain usually do not divide and thus are rarely labeled by BrdU, we further investigated the BrdU effect in cultured astrocytes *in vitro*, because they have a high proliferative capability. Consistent with our *in vivo* findings, we found that BrdU treatment significantly inhibited AtN conversion in cultured astrocytes *in vitro*. Therefore, while BrdU labeling is a useful tool for tracking dividing cells, its potential side effects on cell reprogramming should be thoroughly investigated.

Toxic effects of BrdU on neural stem cells have been widely reported before

Surprised by the unexpected finding that BrdU inhibited AtN conversion, we examined the literature on neural stem cell labeling by BrdU both in the embryonic stage and the adult neurogenesis stage. Not surprisingly, ample studies already report toxic effects of BrdU on neural stem cells both *in vitro* and *in vivo* (Caldwell et al., 2005; Ross et al., 2008; Duque and Rakic, 2011; Lehner et al., 2011; Schneider and d'Adda di Fagagna, 2012). One thorough study by the neurobiologist Pasko Rakic's group on non-human primates detailed the damaging effects of BrdU labeling on neural stem cell differentiation and survival, as well as cell migration and function (Duque and Rakic, 2011). As a halogen-containing thymidine analogue that incorporates into replicating DNA, BrdU has genotoxic side effects. It has been recognized to cause chromosomal constrictions and generate anti-proliferative DNA cross-links (Kaback et al., 1964; Palmer, 1970; Berry and Kinsella, 2001). Another study investigated the molecular mechanisms of the BrdU toxic effects and revealed a systemic loss of DNA methylation with BrdU incorporation into the DNA (Schneider and d'Adda di

Fagagna, 2012). Interestingly, the investigators also found that BrdU incorporation into neural stem cells promoted their differentiation toward astrocytes (Schneider and d'Adda di Fagagna, 2012). How do these studies on BrdU labeling of neural stem cells potentially explain our observation of BrdU-mediated inhibition of AtN conversion? A possible link is the DNA methylation loss upon BrdU incorporation into the DNA (Schneider and d'Adda di Fagagna, 2012). AtN conversion mediated by neural transcription factors depends on the chromatin accessibility of the promoter and enhancer regions of many neuronal genes (Pataskar et al., 2016). If BrdU changes the landscape of DNA methylation during AtN conversion, the reprogramming process may not be completed as usual, leading to a chaotic transcriptomic profile that is neither astrocytic nor neuronal and ultimately to cell death. This may explain why we observed gradual loss of BrdU-labeled astrocytes both *in vitro* and *in vivo* during NeuroD1-mediated AtN conversion. However, this hypothesis requires further investigation.

Besides its effect on DNA methylation, BrdU has been reported to be toxic to neurons by reducing extracellular signal-regulated kinase (ERK) phosphorylation (Caldwell et al., 2005). Our *in vitro* data showed that very few neurons were converted from the BrdU-treated astrocytes compared with the number of neurons converted from untreated astrocytes. Further examination is required to determine whether the BrdU-induced decrease in ERK phosphorylation leads to the low yield of reprogrammed neurons. Additionally, among the BrdU-treated astrocytes, about 30% were not labeled with BrdU. We found that although the AtN conversion rate of this portion of astrocytes was relatively higher than that of the BrdU-labeled astrocytes, it was lower than the conversion rate of the untreated astrocytes. This result suggests that BrdU has a non-autonomous (or indirect) effect on AtN conversion.

BrdU labeling outcome depends on direct AtN conversion or indirect conversion through the neuroprogenitor stage

It is important to emphasize that astrocytes that are directly converted into neurons yield quite different BrdU labeling in the progeny compared with astrocytes that go through the proliferative progenitor stage. For example, during NeuroD1-mediated AtN conversion, astrocytes are directly converted into neurons (Guo et al., 2014; Chen et al., 2020; Zhang et al., 2020). BrdU incorporation may affect the neuronal gene transcription and subsequent translation, leading to incomplete reprogramming and cell death as reported in this study. However, if astrocytes are dedifferentiated into proliferative neuroprogenitors such as astrocytes induced by Sox2 (Niu et al., 2013, 2015; Su et al., 2014; Wang et al., 2016), BrdU would extensively label all the progenitor cells; thus, even if some of them die, it would not be easily noticed. In fact, it is unknown how many dividing progenitors would be generated after Sox2 expression in astrocytes. Therefore, it is expected that Sox2 would have a very different effect from the NeuroD1 effect on BrdU labeling because Sox2-mediated reprogramming occurs through the dividing neuroblast stage, whereas NeuroD1 directly converts astrocytes into neurons without going through the neural stem cell stage (Niu et al., 2013; Guo et al., 2014). This difference should not be viewed as specific to these two transcription factors, but rather applicable to general principles regarding whether astrocytes are directly or indirectly converted into neurons.

BrdU labeling before or after AtN conversion complicates data interpretation

Our finding of BrdU inhibiting AtN conversion raises an important question regarding BrdU labeling before or after AtN conversion, which may result in a different interpretation of the conversion data. For example, in Sox2-induced conversion experiments, BrdU was administrated after the Sox2 transduction and continued for a couple of weeks (Niu et al., 2013, 2015; Su et al., 2014; Wang et al., 2016, 2020). Because Sox2-converted neuroblasts were highly proliferative and able to incorporate BrdU, such long-term administration of BrdU would result in a significant number of BrdU-labeled neurons; however this does not elucidate whether BrdU has detrimental effects. To accurately investigate whether BrdU has inhibitory effects on Sox2-induced cell conversion, BrdU should be administered before Sox2 transduction, not after. Further investigation of the BrdU effect on Sox2 and other transcription factor-induced cell conversion can also be performed in *in vitro* cultured astrocytes as shown in this study.

Conclusion

Our *in vivo* and *in vitro* experiments revealed an unexpected inhibitory effect of BrdU on AtN conversion. BrdU impaired the conversion efficiency and yield of new neurons. Our results suggest that the BrdU-labeling strategy should be used with great caution when conducting AtN conversion experiments.

Acknowledgments: *We thank Ms. Min-Hui Liu, Mr. Liang Xu and Ms. Yu-Ge Xu from Guangdong-Hong Kong-Macau Institute of CNS Regeneration (GHMICR) at Jinan University for issue discussion and valuable suggestions.*
Author contributions: *Study conception and design: WL, GC, TW, JCL; study implementation: TW, JCL; study assistance: WL, XW, QSW, KYW, YYY, QH, JXZ; data analysis: TW, JCL, WL, GC; manuscript drafting: WL, GC, TW. All authors approved the final version of the manuscript.*
Conflicts of interest: *GC is a co-founder of NeuExcell Therapeutics Inc. The other authors have no conflict of interest.*
Financial support: *This study was supported by the Natural Science Foundation of Guangdong Province of China, Nos. 2021A1515011237 (to WL), 2020A1515010854 (to QSW); the National Natural Science Foundation of China, Nos. U1801681 (to GC), 31701291 (to WL); and the Guangdong Province Science and Technology Planning Project of China, No. 2018B030332001 (to GC). The funders had no roles in the study design, conduction of experiment, data collection and analysis, decision to publish, or preparation of the manuscript.*
Institutional review board statement: *The study was approved by Jinan University Institutional Animal Care and Use Committee with approval No. IACUC-20180330-06 on March 30, 2018 for the in vivo experiments and IACUC-20180319-05 on March 19, 2018 for the in vitro experiments.*

Data sharing statement: *Datasets analyzed during the current study are available from the corresponding author on reasonable request.*
Plagiarism check: *Checked twice by iThenticate.*
Peer review: *Externally peer reviewed.*

Open peer reviewer: *Elisabetta Coppi, Universita degli Studi di Firenze, Italy.*
Additional file: *Open peer review report 1.*

References

Agnish ND, Kochhar DM (1976) Direct exposure of postimplantation mouse embryos to 5-bromodeoxyuridine in vitro and its effect on subsequent chondrogenesis in the limbs. J Embryol Exp Morphol 36:623-638.
Ahuja CS, Wilson JR, Nori S, Kotter MRN, Druschel C, Curt A, Fehlings MG (2017) Traumatic spinal cord injury. Nat Rev Dis Primers 3:17018.
Barasch JM, Bressler RS (1977) The effect of 5-bromodeoxyuridine on the postnatal development of the rat testis. J Exp Zool 200:1-8.
Berry SE, Kinsella TJ (2001) Targeting DNA mismatch repair for radiosensitization. Semin Radiat Oncol 11:300-315.
Bond AM, Ming GL, Song H (2015) Adult mammalian neural stem cells and neurogenesis: five decades later. Cell Stem Cell 17:385-395.
Boutin C, Hardt O, de Chevigny A, Coré N, Goebbels S, Seidenfaden R, Bosio A, Cremer H (2010) NeuroD1 induces terminal neuronal differentiation in olfactory neurogenesis. Proc Natl Acad Sci U S A 107:1201-1206.
Burda JE, Sofroniew MV (2014) Reactive gliosis and the multicellular response to CNS damage and disease. Neuron 81:229-248.

Caldwell MA, He X, Svendsen CN (2005) 5-Bromo-2′-deoxyuridine is selectively toxic to neuronal precursors in vitro. Eur J Neurosci 22:2965-2970.
Chen G, Wernig M, Berninger B, Nakafuku M, Parmar M, Zhang CL (2015) In vivo reprogramming for brain and spinal cord repair. eNeuro 2:ENEURO.0106-0115.2015.
Chen YC, Ma NX, Pei ZF, Wu Z, Do-Monte FH, Keefe S, Yellin E, Chen MS, Yin JC, Lee G, Minier-Toribio A, Hu Y, Bai YT, Lee K, Quirk GJ, Chen G (2020) A NeuroD1 AAV-based gene therapy for functional brain repair after ischemic injury through in vivo astrocyte-to-neuron conversion. Mol Ther 28:217-234.
Cho JH, Tsai MJ (2004) The role of BETA2/NeuroD1 in the development of the nervous system. Mol Neurobiol 30:35-47.
Donnan GA, Fisher M, Macleod M, Davis SM (2008) Stroke. Lancet 371:1612-1623.
Duque A, Rakic P (2011) Different effects of bromodeoxyuridine and [3H] thymidine incorporation into DNA on cell proliferation, position, and fate. J Neurosci 31:15205-15217.
Gao Z, Ure K, Ables JL, Lagace DC, Nave KA, Goebbels S, Eisch AJ, Hsieh J (2009) Neurod1 is essential for the survival and maturation of adult-born neurons. Nat Neurosci 12:1090-1092.
Garner W (1974) The effect of 5-bromodeoxyuridine on early mouse embryos in vitro. J Embryol Exp Morphol 32:849-855.
Gascón S, Murenu E, Masserdotti G, Ortega F, Russo GL, Petrik D, Deshpande A, Heinrich C, Karow M, Robertson SP, Schroeder T, Beckers J, Irmler M, Berndt C, Angeli JP, Conrad M, Berninger B, Götz M (2016) Identification and successful negotiation of a metabolic checkpoint in direct neuronal reprogramming. Cell Stem Cell 18:396-409.
Ge LJ, Yang FH, Li W, Wang T, Lin Y, Feng J, Chen NH, Jiang M, Wang JH, Hu XT, Chen G (2020) In vivo neuroregeneration to treat ischemic stroke through NeuroD1 AAV-based gene therapy in adult non-human primates. Front Cell Dev Biol 8:590008.
Guo Z, Zhang L, Wu Z, Chen Y, Wang F, Chen G (2014) In vivo direct reprogramming of reactive glial cells into functional neurons after brain injury and in an Alzheimer's disease model. Cell Stem Cell 14:188-202.
Hancock A, Priester C, Kidder E, Keith JR (2009) Does 5-bromo-2′-deoxyuridine (BrdU) disrupt cell proliferation and neuronal maturation in the adult rat hippocampus in vivo? Behav Brain Res 199:218-221.
Heinrich C, Spagnoli FM, Berninger B (2015) In vivo reprogramming for tissue repair. Nat Cell Biol 17:204-211.
Hevner RF, Hodge RD, Daza RA, Englund C (2006) Transcription factors in glutamatergic neurogenesis: conserved programs in neocortex, cerebellum, and adult hippocampus. Neurosci Res 55:223-233.
Kaback MM, Saksela E, Mellman WJ (1964) The effect of 5-bromodeoxyuridine on human chromosomes. Exp Cell Res 34:182-186.
Kriegstein A, Alvarez-Buylla A (2009) The glial nature of embryonic and adult neural stem cells. Annu Rev Neurosci 32:149-184.
Lehner B, Sandner B, Marschallinger J, Lehner C, Furtner T, Couillard-Despres S, Rivera FJ, Brockhoff G, Bauer HC, Weidner N, Aigner L (2011) The dark side of BrdU in neural stem cell biology: detrimental effects on cell cycle, differentiation and survival. Cell Tissue Res 345:313-328.
Lei W, Li W, Ge L, Chen G (2019) Non-engineered and engineered adult neurogenesis in mammalian brains. Front Neurosci 13:131.
Li H, Chen G (2016) In vivo reprogramming for CNS repair: regenerating neurons from endogenous glial cells. Neuron 91:728-738.
Liu MH, Li W, Zheng JJ, Xu YG, He Q, Chen G (2020) Differential neuronal reprogramming induced by NeuroD1 from astrocytes in grey matter versus white matter. Neural Regen Res 15:342-351.
Liu Y, Miao Q, Yuan J, Han S, Zhang P, Li S, Rao Z, Zhao W, Ye Q, Geng J, Zhang X, Cheng L (2015) Ascl1 converts dorsal midbrain astrocytes into functional neurons in vivo. J Neurosci 35:9336-9355.
Magnusson JP, Goritz C, Tatarishvili J, Dias DO, Smith EM, Lindvall O, Kokaia Z, Frisen J (2014) A latent neurogenic program in astrocytes regulated by Notch signaling in the mouse. Science 346:237-241.
Mattugini N, Bocchi R, Scheuss V, Russo GL, Torper O, Lao CL, Götz M (2019) Inducing different neuronal subtypes from astrocytes in the injured mouse cerebral cortex. Neuron 103:1086-1095.e5.
Miller MW, Nowakowski RS (1988) Use of bromodeoxyuridine-immunohistochemistry to examine the proliferation, migration and time of origin of cells in the central nervous system. Brain Res 457:44-52.
Niu W, Zang T, Zou Y, Fang S, Smith DK, Bachoo R, Zhang CL (2013) In vivo reprogramming of astrocytes to neuroblasts in the adult brain. Nat Cell Biol 15:1164-1175.
Niu W, Zang T, Smith DK, Vue TY, Zou Y, Bachoo R, Johnson JE, Zhang CL (2015) SOX2 reprograms resident astrocytes into neural progenitors in the adult brain. Stem Cell Reports 4:780-794.
Nowakowski RS, Lewin SB, Miller MW (1989) Bromodeoxyuridine immunohistochemical determination of the lengths of the cell cycle and the DNA-synthetic phase for an anatomically defined population. J Neurocytol 18:311-318.
Palmer CG (1970) 5-bromodeoxyuridine-induced constrictions in human chromosomes. Can J Genet Cytol 12:816-830.
Pataskar A, Jung J, Smialowski P, Noack F, Calegari F, Straub T, Tiwari VK (2016) NeuroD1 reprograms chromatin and transcription factor landscapes to induce the neuronal program. EMBO J 35:24-45.
Pollard DR, Baran MM, Bachvarova R (1976) The effect of 5-bromodeoxyuridine on cell division and differentiation of preimplantation mouse embryos. J Embryol Exp Morphol 35:169-178.
Puls B, Ding Y, Zhang F, Pan M, Lei Z, Pei Z, Jiang M, Bai Y, Forsyth C, Metzger M, Rana T, Zhang L, Ding X, Keefe M, Cai A, Redilla A, Lai M, He K, Li H, Chen G (2020) Regeneration of functional neurons after spinal cord injury via in situ NeuroD1-mediated astrocyte-to-neuron conversion. Front Cell Dev Biol 8:591883.
Qian H, Kang X, Hu J, Zhang D, Liang Z, Meng F, Zhang X, Xue Y, Maimon R, Dowdy SF, Devaraj NK, Zhou Z, Mobley WC, Cleveland DW, Fu XD (2020) Reversing a model of Parkinson's disease with in situ converted nigral neurons. Nature 582:550-556.
Rivetti di Val Cervo P, Romanov RA, Spigolon G, Masini D, Martín-Montañez E, Toledo EM, La Manno G, Feyder M, Pifl C, Ng YH, Sánchez SP, Linnarsson S, Wernig M, Harkany T, Fisone G, Arenas E (2017) Induction of functional dopamine neurons from human astrocytes in vitro and mouse astrocytes in a Parkinson's disease model. Nat Biotechnol 35:444-452.
Robel S, Berninger B, Götz M (2011) The stem cell potential of glia: lessons from reactive gliosis. Nat Rev Neurosci 12:88-104.
Roome RB, Bartlett RF, Jeffers M, Xiong J, Corbett D, Vanderluit JL (2014) A reproducible Endothelin-1 model of forelimb motor cortex stroke in the mouse. J Neurosci Methods 233:34-44.
Ross HH, Levkoff LH, Marshall GP, 2nd, Caldeira M, Steindler DA, Reynolds BA, Laywell ED (2008) Bromodeoxyuridine induces senescence in neural stem and progenitor cells. Stem Cells 26:3218-3227.
Ross SE, Greenberg ME, Stiles CD (2003) Basic helix-loop-helix factors in cortical development. Neuron 39:13-25.
Scheltens P, Blennow K, Breteler MM, de Strooper B, Frisoni GB, Salloway S, Van der Flier WM (2016) Alzheimer's disease. Lancet 388:505-517.
Schneider L, d'Adda di Fagagna F (2012) Neural stem cells exposed to BrdU lose their global DNA methylation and undergo astrocytic differentiation. Nucleic Acids Res 40:5332-5342.
Seo S, Lim JW, Yellajoshyula D, Chang LW, Kroll KL (2007) Neurogenin and NeuroD direct transcriptional targets and their regulatory enhancers. EMBO J 26:5093-5108.
Shulman JM, De Jager PL, Feany MB (2011) Parkinson's disease: genetics and pathogenesis. Annu Rev Pathol 6:193-222.
Su Z, Niu W, Liu ML, Zou Y, Zhang CL (2014) In vivo conversion of astrocytes to neurons in the injured adult spinal cord. Nat Commun 5:3338.
Wang LL, Garcia CS, Zhong X, Ma S, Zhang CL (2020) Rapid and efficient in vivo astrocyte-to-neuron conversion with regional identity and connectivity? bioRxiv doi:10.1101/2020.08.16.253195.
Wang LL, Su Z, Tai W, Zou Y, Xu XM, Zhang CL (2016) The p53 pathway controls SOX2-mediated reprogramming in the adult mouse spinal cord. Cell Rep 17:891-903.
Wu Z, Parry M, Hou XY, Liu MH, Wang H, Cain R, Pei ZF, Chen YC, Guo ZY, Abhijeet S, Chen G (2020) Gene therapy conversion of striatal astrocytes into GABAergic neurons in mouse models of Huntington's disease. Nat Commun 11:1105.
Xiang Z, Xu L, Liu M, Wang Q, Li W, Lei W, Chen G (2021) Lineage tracing of direct astrocyte-to-neuron conversion in the mouse cortex. Neural Regen Res 16:750-756.
Zamboni M, Llorens-Bobadilla E, Magnusson JP, Frisén J (2020) A widespread neurogenic potential of neocortical astrocytes is induced by injury. Cell Stem Cell 27:605-617.e5.
Zhang L, Yin JC, Yeh H, Ma NX, Lee G, Chen XA, Wang Y, Lin L, Chen L, Jin P, Wu GY, Chen G (2015) Small molecules efficiently reprogram human astroglial cells into functional neurons. Cell Stem Cell 17:735-747.
Zhang L, Lei Z, Guo Z, Pei Z, Chen Y, Zhang F, Cai A, Mok G, Lee G, Swaminathan V, Wang F, Bai Y, Chen G (2020) Development of neuroregenerative gene therapy to reverse glial scar tissue back to neuron-enriched tissue. Front Cell Neurosci 14:594170.

P-Reviewer: Coppi E; C-Editor: Zhao M; S-Editors: Yu J, Li CH; L-Editors: Yu J, Song LP; T-Editor: Jia Y